Systems/Circuits

Hypothalamic Control of Learned Flight Induced by Threat Imminence

Anita Torossian,* Blake A. Miranda,* Fernando M. C. V. Reis, Elizabeth L. Hilgert, Renesh Gudipati, Catherine P. V. Bloom, Weisheng Wang, Peter J. Schuette, and Avishek Adhikari
Department of Psychology, University of California, Los Angeles, California, 90095

Flexible experience-dependent learned escape has paramount survival value. However, flight is generally investigated in the presence of innate threats. To study conditioned escape, we developed a paradigm in which mice learn to escape a moving shock grid, which simulates a naturalistic situation of being chased by a threat. In a single session, mice learn to escape from the shock-delivering moving grid, displaying a "flight upon grid approach" (FUGA). Importantly, this learned flight is also displayed the next day during fear retrieval, in the absence of shock. We reasoned that circuits implicated in escape and learned fear control this behavior. Fittingly, cholecystokinin (cck)-expressing cells in the hypothalamic dorsal premammillary nucleus (PMd-cck neurons) are necessary for escape from innate threats, and PMd activity modulates learned defense, suggesting it may participate in the maintenance of learned FUGA escapes. Here, we show in male and female mice that inhibiting PMd-cck activity during FUGA acquisition impairs learned flight during fear retrieval. Furthermore, these results were specific to a paradigm with a moving threat, as PMd-cck inhibition during fear acquisition did not alter behavior during fear retrieval in contextual or auditory-cued fear conditioning. Lastly, PMd-cck cells encoded distance to the moving grid and FUGA escape speed, but were not activated by fear-conditioned tones or conditioned freezing. These data show that the PMd is critical for the maintenance of the memory of the threat associated with the grid and underscore recent views demonstrating that the hypothalamus has key contributions for learning flexible experience-dependent survival actions.

Key words: **chemogenetics; dorsal premmammillary; escape; flight; hypothalamus; predatory imminence**

Significance Statement

Here, we show the initial characterization of a novel assay that produces learned flight in mice induced by a moving threat. We also demonstrate that activity of the hypothalamic dorsal premammillary nucleus is necessary for the maintenance of this behavior. These data add to the emerging view that the hypothalamus can play potent roles in learning.

Received Sept. 16, 2024; revised March 13, 2025; accepted March 21, 2025.

Author contributions: A.T., F.M.C.V.R., and A.A. designed research; A.T., E.L.H., R.G., C.P.V.B., and W.W. performed research; A.T. and F.M.C.V.R. contributed unpublished reagents/analytic tools; A.T., B.A.M., P.J.S., and A.A. analyzed data; A.T., B.A.M., and A.A. wrote the paper.

A.T. was supported by F31MH127943-01A1. This work was supported by the National Institute for Mental Health (R00 MH106649 and R01 MH119089 to A.A.), the National Diabetes and Digestive and Kidney Diseases (R01DK139605 to A.A.), the Hellman Foundation (to AA), the Brain & Behavior Research Foundation (Grant No. 22663 to AA and Grant Nos. 27654 and 31093 to F.M.C.V.R.), the National Science Foundation (NSF-GRFP to P.J.S. and B.A.M.), the UCLA Affiliates fellowship (to P.J.S.), and the Eugene Cota-Robles Award (to B.A.M.). Research reported in this publication was supported by the National Institute of Diabetes and Digestive and Kidney Diseases (NIDDK), the Office of Disease Prevention (ODP), the Office of Nutrition Research (ONR), the Chief Officer for Scientific Workforce Diversity (COSWD), and the Office of Behavioral and Social Sciences Research (OBSSR) of the National Institutes of Health under Award Number U24DK132746-01, UCLA LIFT-UP (Leveraging Institutional support for Talented, Underrepresented Physicians and/or Scientists). The content is solely the responsibility of the authors and does not necessarily represent the official views of the National Institutes of Health. We thank Judy Genshaft and Steven Greenbaum for funding the 2022 Young Investigator Award (Grant No. 31093), The Nancy and Jon Glaser Family Friends of Semel Scholar Award, and the UCLA LIFT-UP Award (to F.M.C.V.R.).

*A.T. and B.A.M. contributed equally to this work.

The authors declare no competing financial interests.

Correspondence should be addressed to Avishek Adhikari at avi@psych.ucla.edu.

https://doi.org/10.1523/JNEUROSCI.1806-24.2025

Introduction

Animals display a constellation of defensive actions to decrease threat exposure, including freezing and escape (McNaughton and Corr, 2004). Fear conditioning studies (Johansen et al., 2010) have revealed invaluable insights about the acquisition and retrieval of conditioned freezing (Maren, 2001). However, escape has mostly been studied with innate threats (Wirsing et al., 2010; Shang et al., 2018; Tobias et al., 2023), even though learning to escape during cues associated with high-imminence threats is valuable and adaptive.

Learned flight has been studied mostly with the two-way signaled active avoidance (shuttlebox) assay (Johansen et al., 2010; Jercog et al., 2021). More recently, researchers developed a promising assay using a serial compound auditory stimulus of tone and white noise (Borkar et al., 2020, 2024). The white noise elicited learned escape after fear acquisition. While these assays have generated valuable insights, an important consideration is that a common cause for escape in rodents is chase by a concrete threat, such as a predator (Wirsing et al., 2010).

However, the paradigms above do not simulate naturalistic chase. Pursuit by an aerial predator can be simulated by looming stimuli, but the induced innate defensive actions cannot be seen in most animals by the second trial (Yilmaz and Meister, 2013). There are also assays that simulate chase with robotic predators. These assays elicit escape (Choi and Kim, 2010; Amir et al., 2015; Tsutsui-Kimura et al., 2022; Han et al., 2023; Lai et al., 2024) and inhibit foraging while the robot is moving. However, robotic predator-induced escape occurs in the first exposure. Consequently, these assays cannot be used to study learned escape. Thus, there is no widely used task that elicits conditioned escape caused by a simulated predator pursuit.

Predatory pursuit alters threat proximity, which is a cardinal determinant of high predatory imminence leading to flight (Perusini and Fanselow, 2015). To study learning of flight, we developed an assay in which predatory pursuit is simulated by movement of a shocking grid. Mice learn in a single session to quickly traverse the moving grid to avoid footshocks, displaying "flight upon grid approach" (FUGA). During fear retrieval the next day, mice display robust FUGA in the absence of shock. We chose the acronym FUGA because it is derived from the Latin "fugere," meaning "to escape." Indeed, escape in modern Romance languages such as Italian, Spanish, and Portuguese is "fuga," and the same root is used in English words such as "fugitive."

Several results indicate that the hypothalamic dorsal premammillary nucleus (PMd) is involved in acquiring learned escapes. First, PMd lesions decrease predator-induced defense (Canteras et al., 1997). Second, activity of cholecystokinin (cck)-expressing PMd cells is necessary and sufficient to promote escape from various innate and learned threats (Wang et al., 2021a,b). There are also tantalizing reports showing PMd involvement in learned defense. For example, PMd inactivation with muscimol diminishes fear in predator-conditioned contexts (Cezario et al., 2008), and PMd-cck chemogenetic inhibition during retrieval of contextual fear conditioning decreases escape vigor elicited by a stationary shock grid (Wang et al., 2021a). Furthermore, PMd activation with a β-adrenergic agonist during a neutral odor presentation induces conditioned odor avoidance (Pavesi et al., 2011). Moreover, PMd-cck inhibition during retrieval increased fear extinction of a footshock-induced contextual fear memory (Viellard et al., 2024). These data indicate that PMd is critical for flight and that it is involved in conditioned defensive actions, suggesting it may participate in the maintenance of learned flight in the FUGA assay.

We show that PMd-cck cell inhibition during fear acquisition impaired FUGA in retrieval. This effect was task-specific, as PMd-cck inhibition during acquisition of auditory or contextual fear conditioning did not impair behavior in retrieval. Furthermore, these cells encoded learned FUGA and movement of the conditioned threat, but they were not activated by a fear-conditioned tone. These data show that the PMd participates in the maintenance of learned flight or supports the memory of the grid's threat level.

Materials and Methods

All procedures conformed to guidelines established by the National Institutes of Health and have been approved by the University of California, Los Angeles Institutional Animal Care and Use Committee, protocols 2017-011 and 2017-075. All procedures conform to ARRIVE guidelines.

Mice. cck-IRES-Cre mice (The Jackson Laboratory stock #012706) and wild-type C57BL/6J mice (The Jackson Laboratory stock #000664) were used for all experiments. Male and female mice between 2 and 6 months of age were used in all experiments. Mice were maintained on a 12 h reverse light/dark cycle with food and water *ad libitum*. Sample sizes were chosen based on previous behavioral optogenetics studies on defensive behaviors, which typically use 6–15 mice per group. All mice were handled for a minimum of 3 d prior to any behavioral task.

Viral vectors. All vectors were purchased from Addgene.

Chemogenetics. AAV8-hSyn-DIO-hM4D(Gi)-mCherry and AAV8-Syn-DIO-mCherry.

Fiber photometry. AAV9-Syn-FLEX-GCaMP6s-WPRE-SV40.

Surgeries. Eight-week-old mice were anesthetized with 1.5–3.0% isoflurane and placed in a stereotaxic apparatus (Kopf Instruments). A scalpel was used to open an incision along the midline to expose the skull. After performing a craniotomy, 40 nl of one of the viral vectors listed above at a titer of 2×10^{12} particles/ml was injected using a 10 µl NanoFil syringe (World Precision Instruments) at 0.08 µl/min. AAV8-hSyn-DIO-hM4D(Gi)-mCherry and AAV8-hSyn-DIO-mCherry were injected at a titer of 2×10^{12} particles/ml as reported (Tobias et al., 2023; Reis et al., 2024). The syringe was coupled to a 33-gauge beveled needle, and the bevel was placed to face the anterior side of the animal. The syringe was slowly retracted 20 min after the start of the infusion. Mice received unilateral viral infusion and fiber-optic cannula implantation. Infusion locations measured as anteroposterior, mediolateral, and dorsoventral coordinates from bregma were as follows: dorsal PMd (−2.46, −0.5, −5.35). For optogenetic experiments, fiber-optic cannula (0.22 NA, 200 µm diameter; Newdoon) were implanted bilaterally 0.15 mm above the viral infusion sites. Only mice with viral expression restricted to the intended targets were used for behavioral assays.

For photometry experiments, mice were injected with 0.16 µl at a titer of 3×10^{12} of AAV9.Syn.Flex.GCaMP6s.WPRE.SV40 in the PMd of cck-cre mice. Mice were implanted unilaterally with fiber-optic cannulae in the PMd. A 400-µm-diameter, 0.48 NA optical fiber (Neurophotometrics) was used for photometry experiments. Adhesive cement (C&B Metabond; Parkell) and dental cement (Stoelting) were used to securely attach the fiber-optic cannula to the skull.

Flight upon grid approach (FUGA) assay. The experimental setup consisted of a 77 × 15 cm floor area and 40 cm height chamber with a shock grid (16.5 × 15 cm) positioned at one end. A Coulbourn Instruments mouse shock grid was used. During the initial 10 min exploration period, mice were allowed free movement in the chamber. The shock grid was present but did not deliver shocks or move during this period. In the habituation phase (15 min), the shock grid was moved by the experimenter across the chamber at a rate of 8.5 cm/s, traversing the grid in 9 s. After each movement, the grid paused for a variable stationary intertrial period of 15–25 s. Each movement from one side to the other constituted one trial, with a total of 22 trials per session, divided into two blocks of 11 trials with an 85 s interblock interval.

On the shock day (20 min) there were 33 trials, divided into three blocks of 11 trials with 85 s interblock intervals. The shock grid was active (delivering 0.6 mA shocks continuously) only during the second block of 11 trials (Trials 12–22). The shock grid was off during the other trials (Trials 1–11 and 23–33).

Twenty-four hours later, on the fear retrieval day, mice were exposed to 33 grid movements without shocks, following the same protocol as shock day, but with the shock grid turned off.

Stationary shock grid assay. The chamber setup was similar to the FUGA assay (same dimension of 77 × 15 cm chamber with 40 cm high walls). The same 16.5 × 15 cm shock grid used in FUGA was placed at one end of the chamber. The shock grid, however, was stationary across all sessions. All sessions of this experiment were held for 10 min. Mice were given two habituation days to acclimate to the enclosure. On shock day, mice freely explored the environment and received a 0.6 mA shock the first two times they were fully on the grid (all four paws were on the grid). The grid was turned off after two shocks were delivered. A 10 min retrieval day without shock was given 24 h later.

Auditory fear conditioning. Mice were conditioned in standard Coulbourn Instruments mouse fear conditioning chambers with a floor shock grid area of 17 by 20 cm and a height of 28 cm. The auditory stimulus used was a pure sinusoidal tone of 10 s, 2,900 Hz, and 80 dB intensity. During habituation day, mice were exposed to five tone trials, with a variable intertrial interval between 60 and 100 s. On shock day 24 h later, five 10 s tones were delivered that coterminated with a shock (0.6 mA, 1 s). The environment was then altered to isolate cued freezing from contextual freezing. We placed a white semicircular insert for the walls, a white insert for the floor with scattered bedding, and 20% vinegar solution underneath the chamber floor and added white noise (70 dB) 4 ft away from the conditioning chambers. To further ensure the novelty of the context, mice were transported to the experimental room by hand from opposing hallway directions. Mice were habituated to this environment for 60 min, 24 h after shock day. The next day, mice were placed in this environment, and five tones were delivered. The tone, habituation, and shock sessions lasted 9 min, and the novel context habituation lasted 60 min. Freezing levels during tone were determined by the software FreezeFrame (Actimetrics). Baseline freezing was measured in the period of 124 s preceding the first tone of each session.

Chemogenetics. Mice used for FUGA, stationary grid, and auditory fear conditioning assays were all given clozapine N-oxide (CNO; 5 mg/kg) injected intraperitoneally 40 min prior to fear acquisition sessions, as reported (Wang et al., 2021a). CNO was only administered during test days for all experiments. Separate cohorts of mice were used for each behavior assay.

Fiber photometry. Photometry was performed as described (Wang et al., 2021a). Briefly, we used a 405 nm LED and a 470 nm LED (Thorlabs, M405F1 and M470F1) for the Ca^{2+}-dependent and Ca^{2+}-independent isosbestic control measurements. The two LEDs were bandpass filtered (Thorlabs, FB410-10 and FB470-10) and then combined with a 425 nm low-pass dichroic mirror (Thorlabs, DMLP425R) and coupled into the microscope using a 495 nm low-pass dichroic mirror (Semrock, FF495-Di02-25 × 36). Mice were connected with a patch cord (400 μm, Doric Lenses) using a zirconia sleeve to the optical system. The signal was captured at 20 Hz (alternating 405 nm LED and 470 nm LED). To correct for signal artifacts of a nonbiological origin (i.e., photobleaching and movement artifacts), custom MATLAB scripts leveraged the reference signal (405 nm), unaffected by calcium saturation, to isolate and remove these effects from the calcium signal (470 nm).

Behavioral quantification. To extract the pose of freely behaving animals in the described assays, we implemented DeepLabCut (Mathis et al., 2018), an open-source convolutional neural network-based toolbox, to identify mouse nose, ear, and tail base x–y coordinates in each recorded video frame. These coordinates were then used to calculate speed and position at each time point.

"Flight upon grid approach (FUGA)" behaviors were separated into either "successful" or "failed" FUGA types. Successful FUGAs were defined as epochs for which (1) the shock grid was in motion, (2) the mouse completely traversed the shock grid opposite the grid's direction of movement, (3) the traversal occurred at a mean speed exceeding a minimum threshold of 3.7 cm/s, and (4) the total traversal time was ≤1 s. Trials that did not satisfy all of these successful FUGA criteria were classified as failed FUGA.

"Freezes" were defined as epochs when head and tailbase velocities fell below 0.25 cm/s for a period of at least 0.33 s.

"Approaches" were defined as epochs for which (1) the mouse moved toward the shock grid at a speed exceeding a minimum threshold of 3 cm/s and (2) the distance traveled between approach onset and offset exceeded at least 10 cm. If the grid was in motion, approach epochs were designated only if the grid was >5 cm away from the mouse at the start of the behavior. There was little room for acceleration toward the shock grid if the mouse was located against the opposite wall near the end of the shock grid's movement, requiring a relatively lowered distance threshold for detection during these instances.

"Retreats" were defined as epochs for which (1) the mouse moved away from the shock grid at a speed exceeding a minimum threshold of 3 cm/s, (2) the mouse did not traverse the shock grid (if it was in motion), and (3) movement in the opposite direction initiated <30 cm away from the shock grid.

"Stretch-attend postures" were defined as epochs for which (1) the distance between mouse nose and tailbase exceeded a distance of approximately 1.2 mouse body lengths and (2) mouse tailbase speed fell below 1 cm/s.

Statistics. Nonparametric two-tailed Wilcoxon signed rank or rank sum tests were used, unless otherwise stated using MATLAB. Two-tailed tests were used throughout with $\alpha = 0.05$. Asterisks in plots indicate the p values. The standard error of the mean was plotted in each figure as an estimate of variation. When applicable, multiple comparisons were adjusted with the false discovery rate method. All error bars in all plots represent the standard error of the mean.

Results

In order to study conditioned flight that is elicited by higher threat imminence, we developed the FUGA assay using a moving shock grid as a conditioned threat. Shock grids have been used to generate contextual conditioning for many years (Fanselow, 2010), but in previous studies, the grid was always immobile, and thus the only parameter that could alter threat imminence was the intensity or frequency of the shock delivery. Here, we altered this model, and instead parametrically changed the threat imminence of the grid by moving it toward the mouse along a corridor (Fig. 1). Mice were first placed in a long rectangular chamber containing an inactive shock grid that is turned off. The grid was moved back and forth (left to right and vice versa) throughout the length of the rectangular chamber. Each movement traversing the chamber once in a single direction constituted one trial. During habituation, the mouse was exposed to 22 grid movement trials in the absence of shock. Habituation was done to measure baseline defensive behaviors to the grid movement prior to fear acquisition. The next day, mice were reexposed to the chamber with 33 trials. The grid was electrically activated (0.6 mA) only during Trials 12–22 on the shock day (fear acquisition; all data hereafter labeled as FUGA "shock" come from these 12–22 trials from shock day). Intertrial intervals ranged from 15 to 85 s. Mice then gradually learned to avoid the shocking grid by rapidly traversing the grid (i.e., flight upon grid approach, or FUGA). If mice failed to do FUGA behavior successfully, an unsuccessful FUGA was scored. The following day, mice were exposed to 33 trials in the absence of shock to measure fear retrieval. Fear learning was evaluated by comparing defensive behaviors across habituation and fear retrieval. Relative to habituation, during retrieval mice displayed an increase in the number of successful FUGA trials (Fig. 2*a*), higher mean and maximum FUGA speed (Fig. 2*c*,*d*), and increased freezing (Fig. 2*e*). During retrieval mice also exhibited decreased time spent on top of the grid, indicating avoidance (Fig. 2*f*). These data indicate that the FUGA assay induces a wide range of defensive behaviors during retrieval, including avoidance and freezing. Most importantly, the assay also induced learned escape triggered by the approach of the moving grid.

In this assay the grid moves, but there are also intertrial intervals during which the grid is not moving. During these immobile stationary grid epochs, mice occasionally approached the grid and then ran away from it. These movements were "retreats" from the grid (Fig. 2*h*). Note that this movement is distinct from FUGA, which occurs when mice rapidly traverse the moving grid (Fig. 1). Importantly, behavior during retrieval did not differ between male and female mice (Extended Data Fig. 2-1), and FUGA escape and freezing remain consistent throughout the entire retrieval session (Extended Data Fig. 2-2).

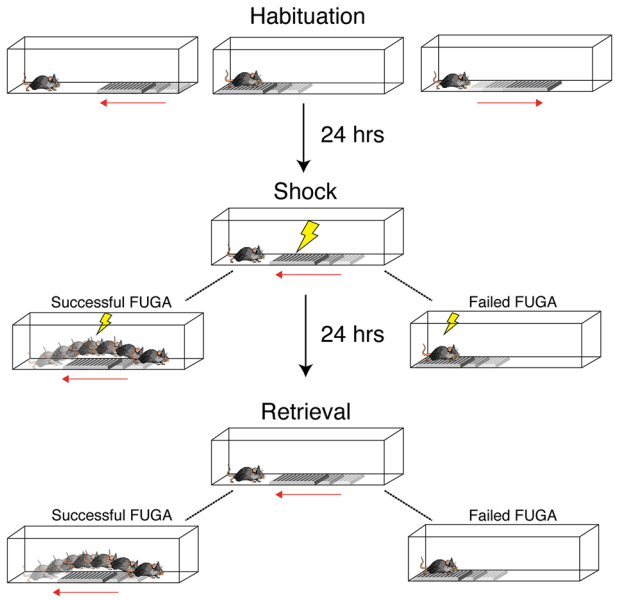

Figure 1. Flight upon grid approach (FUGA) assay can elicit acquisition and retrieval of learned escape. During habituation, a mouse is placed in a long rectangular box. A moveable shocking grid rests at one end of the box. The grid moves from one side to the next and then stays immobile when it reaches the other end of the box. In the example shown, the grid is first moving from right to left and then from left to right. The grid alternates between right–left and left–right movements with stationary resting epochs in between. The grid does not deliver shocks during habituation day. Mice do not show defensive actions or avoidance of the grid during habituation. Twenty-two grid movements happen during habituation day. The next day, the grid moves in the same manner as did during the habituation day, but for 33 trials. The shock grid is turned ON and delivers shocks only during Trials 12–22. The mouse gradually learns to avoid the shocking grid by traversing the grid in the direction opposite to the grid's movement. In this example, the grid is moving toward the left, and the mouse may traverse the grid by rapidly running or jumping over the grid moving toward the right to minimize contact with the grid. If the mouse performs rapid flight upon grid approach (FUGA), the trial is classified as a successful FUGA attempt. If the animal stays on top of the moving grid or otherwise fails to rapidly traverse the grid, the trial is classified as a failed FUGA. Twenty-four hours after the fear acquisition day, a retrieval test is performed with 33 trials, in which the grid again alternates between left–right and right–left movements with stationary periods in between. No shocks are delivered during retrieval day. The mouse performs either successful or failed FUGA trials during each grid movement.

We next investigated neural circuits that affect the maintenance of learned FUGA escapes. We and others showed that activity of hypothalamic PMd-cck cells was necessary for escapes elicited by a variety of innate threats (Wang et al., 2021a,b; de Araujo Salgado et al., 2023), and other reports showed this nucleus also was implicated in learned defensive actions (Do Monte et al., 2008; Pavesi et al., 2011; Wang et al., 2021a). We thus hypothesized that the activity of PMd-cck cells is necessary for the maintenance of FUGA behavior. To test this view, we used cck-cre mice and expressed the inhibitory receptor hM4Di in PMd-cck cells (Fig. 3*a*). The hM4Di ligand clozapine *N*-oxide (CNO) was administered intraperitoneally 40 min prior to fear learning (shock day; Fig. 3*b*). Importantly, both groups performed similarly during habituation and shock day (Extended Data Figs. 3-1 and 3-2). However, marked behavioral differences were seen during fear retrieval. Traces from representative mice indicated that FUGA speed was lower in mice expressing hM4Di in the PMd, compared with control mice (Fig. 3*c*). This finding suggests that inhibition of these cells during fear acquisition impaired FUGA during retrieval. Indeed, chemogenetic inhibition of PMd-cck cells during shock day decreased the number of successful FUGA trials during retrieval (Fig. 3*d*,*e*). Furthermore, during retrieval, mice expressing hM4Di also showed decreased mean and maximum FUGA speed (Fig. 3*f*,*g*) and less freezing (Fig. 3*h*) compared with control mice. These data show that PMd-cck activity during fear acquisition is necessary for displaying FUGA learned escapes the next day in fear retrieval. PMd-cck inhibition immediately after fear acquisition did not cause behavioral impairments during retrieval (Extended Data Fig. 3-3), indicating that the observed effects in Figure 3 are likely not caused by long-lasting effects of CNO that decreased consolidation. We then studied behavioral differences separately in the grid moving epochs and the intertrial moments during which the grid is stationary. Strikingly, PMd-cck inhibition during shock day decreased freezing and time on grid during retrieval day only during grid moving epochs, but not during grid stationary epochs (Extended Data Fig. 3-4*a–e*). PMd inhibition also did not alter anxiety-related behavior and locomotion (Extended Data Fig. 3-4*g*,*h*), in line with our previous data (Wang et al., 2021a,b). These data show that PMd-cck inhibition during fear acquisition preferentially affected defensive behaviors during grid movement epochs in fear retrieval.

The data above indicate that PMd-cck activity during fear acquisition is necessary to perform moving threat-induced FUGA escapes in retrieval. We then studied if PMd-cck activity was required to learn a similar task, but in which the threat is not moving. To do so, we performed the stationary shock grid task, in which the shocking grid is always immobile and is never moved. The same chamber from the FUGA assay was used in this task. During habituation day, mice were placed in a rectangular chamber with a shock grid on the opposite end. Mice freely explored the environment. The next day (shock day or fear acquisition), mice received footshocks each time they voluntarily approached and touched the grid. The following day, during fear retrieval, mice were exposed to the same environment, but the shock grid was turned off. CNO was administered to mice expressing either hM4Di or mCherry in PMd-ccck cells 40 min prior to the shock day session (Fig. 4*a*). Both groups of mice learned to avoid the grid during fear retrieval (Fig. 4*b*). Furthermore, during habituation, shock (Extended Data Fig. 4-1) and retrieval (Fig. 4), both groups of mice displayed similar levels of freezing (Fig. 4*c*), grid avoidance (Fig. 4*d*), and other behaviors (Fig. 4*e–h*). These data show that the activity of PMd-cck cells is not necessary for fear learning in a standard contextual conditioning task in which the grid is not moving.

In the FUGA assay, the conditioned stimulus is a moving shock grid. The grid movement has a well-defined onset and offset, similar to a cue in pavlovian fear. We thus studied if PMd-cck activity was necessary for fear learning in other cued fear tasks. We used an auditory-cued fear task, in which there is a cue, but no moving stimuli. To do so, we investigated if PMd-cck cell activity was necessary for auditory-cued fear conditioning. Mice were exposed to five auditory tones during habituation without shock. The next day, mice were exposed to five tones that coterminated with footshocks (fear acquisition or shock day). Forty-eight hours later, mice were exposed to five tones in the absence of shock to evaluate fear retrieval. CNO was administered to mCherry- or hM4Di-expressing mice 40 min prior to shock day (Fig. 5*a*). Both groups performed similarly and showed robust freezing during retrieval (Fig. 5*b*,*c*), indicating that PMd-cck activity is not necessary for learning cued auditory fear conditioning.

To characterize PMd-cck activity, we expressed the calcium indicator GCaMP6s in these cells (Fig. 6*a*,*b*) and obtained

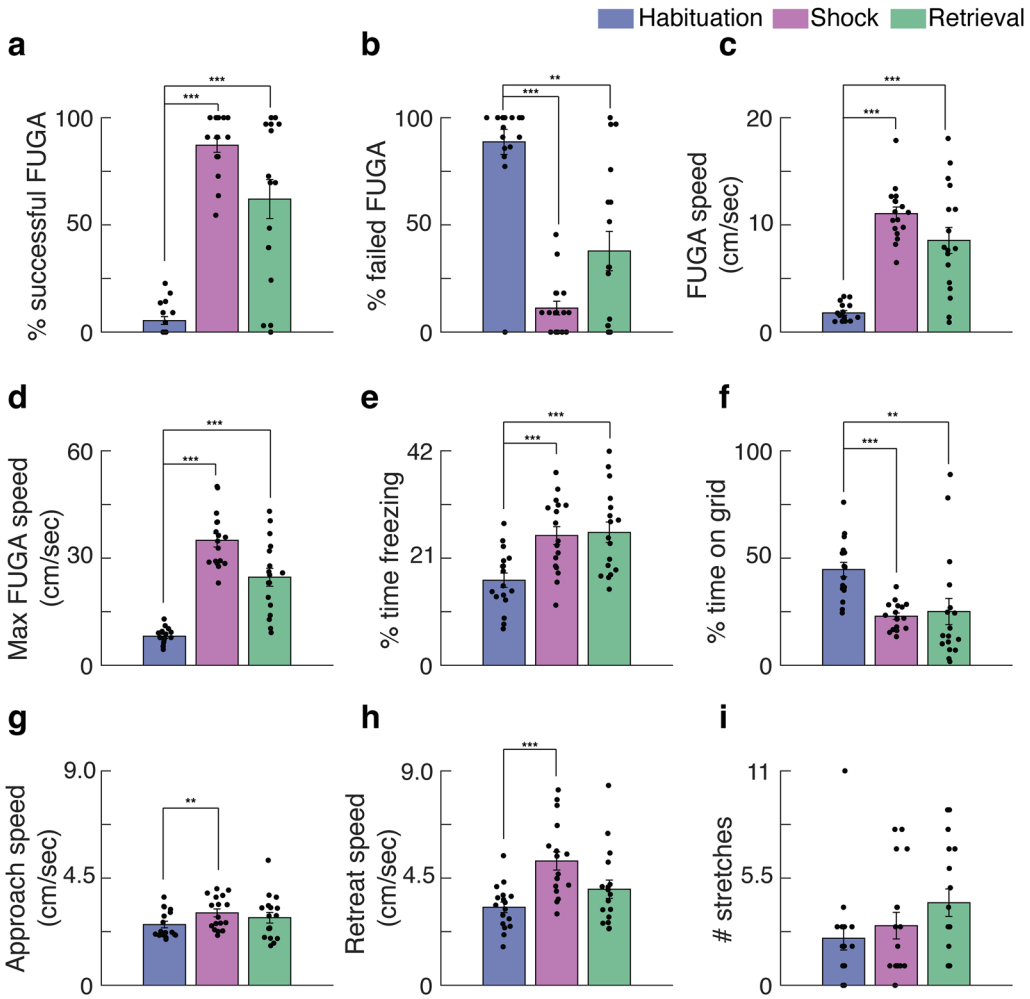

Figure 2. Characterization of mouse behavior in the FUGA assay. Behavioral measures were evaluated in habituation (prior to learning), shock day (fear acquisition), and retrieval. All days are separated by 24 h. To evaluate fear learning, behaviors were compared between habituation and retrieval days. Fear learning caused an increase in % of successful FUGA trials (***a***), a decrease in % of trials with failed FUGA (***b***), an increase in mean (***c***) and maximum (***d***) FUGA speed, an increase in freezing (***e***), and a decrease of time spent on the shock grid (***f***). Approach to grid mouse speed did not change across days (***g***), while retreat speed increased slightly (***h***). The number of stretch-attend risk assessment postures also did not increase across days (***i***). $n = 17$ mice, $*p < 0.05$, $**p < 0.01$, $***p < 0.005$, Wilcoxon sign rank test (Extended Data Figs. 2-1 and 2-2).

recordings of neural activity during auditory fear conditioning. PMd-cck cells were not activated by the auditory tone, neither before nor after fear conditioning (Fig. 6*c–e*), though activation was elicited by the footshock (Fig. 6*d*). Furthermore, PMd activity did not correlate with freezing across trials (Fig. 6*f–h*). These results agree with our data showing that PMd-cck activity is not necessary for learning of the cued auditory fear conditioning task (Fig. 5).

We then investigated PMd-cck activity in the moving grid FUGA assay. We first analyzed the data during the intertrial periods in which the grid was not moving, and we parsed the data into time points when the mouse was facing the grid and moments in which the mouse faced away from the grid (Fig. 7*a*). Interestingly, a negative correlation between PMd-cck activity and distance to the stationary grid was found in retrieval when the mouse faced the grid, which is presumably when the animal is able to visually evaluate this distance (Fig. 7*b*). This correlation was not found when the mouse faced away from the grid (Fig. 7*c*). Moreover, PMd-cck activity is significantly increased when the mouse walks toward the grid, which are moments in which the animal is facing the grid (Fig. 7*e*). Importantly, PMd-cck cells were not activated during movement toward the grid in habituation (Fig. 7*f*).

We next analyzed behavior and PMd-cck activity during grid movement (Fig. 8*a*). Freezing is high during retrieval during the start of the grid movement, but it drops afterward (Fig. 8*b*), as the behavior shifts from freezing to FUGA toward the end of the grid movement (Fig. 8*c*). This shows that on average, animals tend to perform FUGA after several seconds following grid movement onset, when the grid is near the animal. We then investigated if PMd-cck activity was higher during proximity to the moving grid. We only used data points during grid movement that occurred prior to successful FUGA onset, to separate encoding of distance to grid from encoding of FUGA escape. Data from a representative trial (Fig. 8*d*) show that when the grid is moving toward the mouse, PMd-cck neural activity is negatively correlated with distance to threat during retrieval even when restricting the analysis to time points that occur prior to FUGA escape onset (Fig. 8*e*). During the time points used for this analysis, mouse velocity was lower during grid movement in retrieval than in habituation (Fig. 8*f*), due to increased freezing seen in retrieval, but not habituation (Fig. 8*b*; see PMd activity during freezing in Extended Data Figs. 8-1 and 8-2). Thus, PMd-cck activity is correlated with grid proximity in retrieval even when analyzing a time window in which mouse velocity is lower in

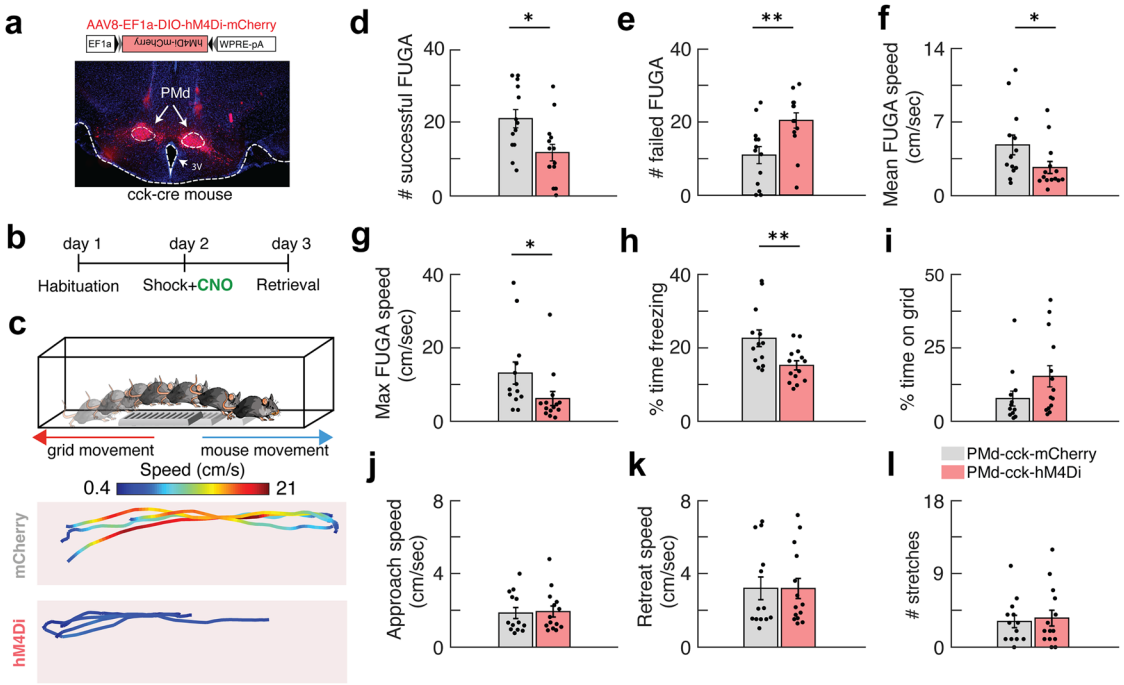

Figure 3. Inhibition of the dorsal premammillary nucleus (PMd) during fear acquisition impairs retrieval of FUGA. ***a***, In order to inhibit the PMd, the inhibitory receptor hM4Di-mcherry was expressed in cholecystokinin (cck)-expressing PMd cells. Top, Scheme of the viral vector used. Bottom, Representative image showing expression of hM4Di-mcherry in the PMd of a cck-cre mouse. ***b***, Timeline of FUGA assay. The hM4Di ligand clozapine *N*-oxide (CNO) was injected intrapertoneally in mice 40 min prior to fear acquisition on shock day. ***c***, Scheme showing a trial with successful FUGA during fear retrieval. The mouse rapidly traverses the grid in the direction opposite of grid movement. The bottom two panels below show tracks of representative fear retrieval FUGA trials in which mice are moving toward the right side to escape from the moving grid. The speed at each location in the track is represented in a heatmap (warmer colors correspond to higher FUGA speed). The example tracks show that inhibition of PMd-cck cells during fear acquisition decreased FUGA speed during fear retrieval. Inhibition of PMd-cck cells during fear acquisition induced several impairments 24 h later during fear retrieval. Data in ***d–l*** are from fear retrieval day. Relative to control mice, PMd-cck hM4di mice showed reduced trials with successful FUGA (***d***; $p = 0.011$), higher number of failed FUGA (***e***; $p = 0.005$), lower mean FUGA speed (***f***; $p = 0.035$), lower maximum FUGA speed (***g***; $p = 0.016$), and reduced freezing (***h***; $p = 0.008$). PMd-cck inhibition during fear acquisition did not alter time spent on top of the grid (***i***; $p = 0.062$) speed of approach (***j***; $p = 0.30$) or non-FUGA retreat from the grid (***k***; $p = 0.78$). Note that retreats are different from FUGA. When the mouse walks toward the grid and then rapidly runs away from it, a retreat is scored. In contrast, FUGA occurs when the grid moves toward the mouse and the mouse rapidly traverses the grid (see scheme in ***c***). The number of stretch-attend postures was also not altered relative to control mice (***l***; $p = 0.99$). ***d–l***, All data are from retrieval day and are plotted as mean ± SEM, $n = 13$ mcherry and 14 hM4Di mice; all p values were obtained from the Wilcoxon rank sum test. *$p < 0.05$, **$p < 0.01$ (Extended Data Figs. 3-1–3-4).

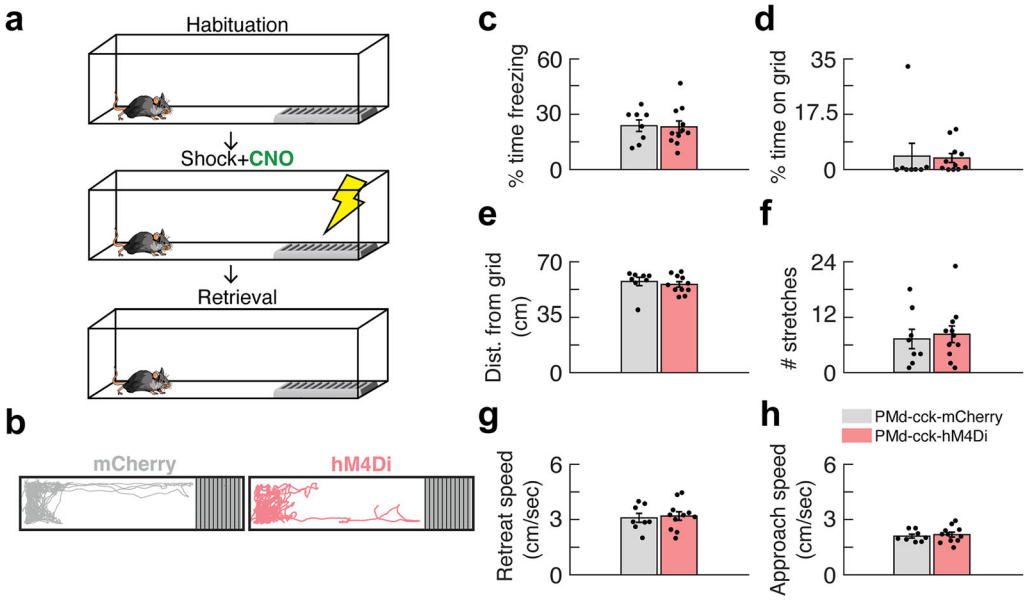

Figure 4. PMd-cck inhibition in fear acquisition of nonmoving stationary grid does not affect behavior during fear retrieval session 24 h later. ***a***, Timeline of stationary grid behavioral assay. Habituation, shock (fear acquisition), and retrieval occurred in 3 consecutive days. CNO was injected in mice 40 min prior to fear acquisition shock day. This shock grid remained stationary during the entire assay and was never moved. Shocks were delivered only on shock day (fear acquisition) if the mouse touched the grid. ***b***, Example behavioral tracks from retrieval session from representative mice expressing either mcherry or hM4Di. Note that both animals avoided the grid (on the right) to a similar degree during the retrieval session. All data in ***c–h*** are from the retrieval session**.** Inhibition of PMd-cck cells during shock (fear acquisition day) did not alter any defensive behaviors on fear retrieval, including freezing ($p = 0.90$; ***c***), time spent on grid ($p = 0.10$; ***d***), distance from grid ($p = 0.10$; ***e***), number of stretch-attend risk assessment postures ($p = 0.62$; ***f***), speed approaching the grid ($p = 0.84$; ***g***), or speed while retreating from the grid ($p = 0.61$; ***h***). ***c–h***, All data are plotted as mean ± SEM, $n = 8$ mcherry and 11 hM4Di mice; all p values were obtained from the Wilcoxon rank sum test (Extended Data Fig. 4-1).

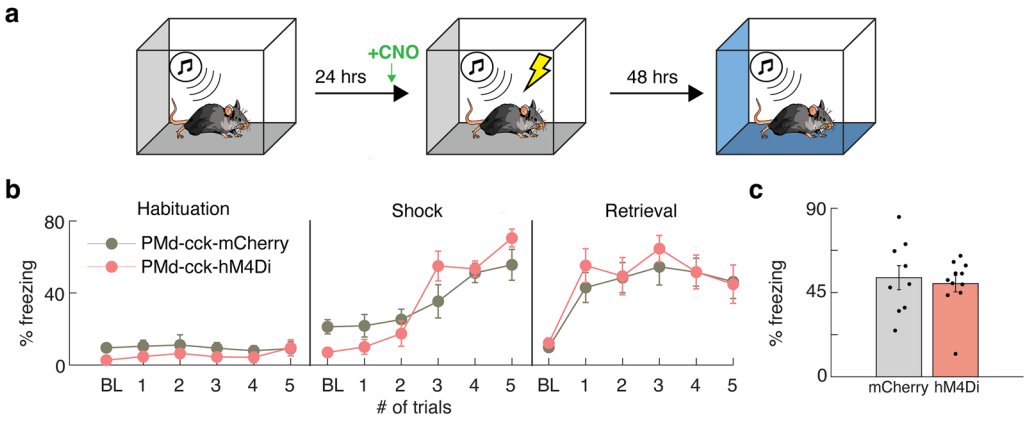

Figure 5. PMd-cck activity during acquisition of cued fear conditioning does not affect freezing during retrieval. ***a***, Scheme showing the behavioral protocol for auditory-cued fear conditioning over 3 d [habituation, shock (fear acquisition), and retrieval]. Habituation and shock occurred in the same context, while retrieval occurred in a different context to isolate cued freezing from contextual freezing. CNO was injected intraperitoneally 40 min prior to shock day (fear acquisition). ***b***, Plot showing freezing for mice expressing control mcherry or hm4Di in PMd-cck cells during the conditioned auditory fear protocol. CNO was administered prior to shock (fear acquisition). Each trial represents one auditory tone. BL, baseline freezing, prior to the first auditory tone of that session. ***c***, There was no significant difference in freezing across groups during fear retrieval ($p = 0.94$, Wilcoxon rank sum test). $n = 9$ mcherry and 11 hM4Di mice.

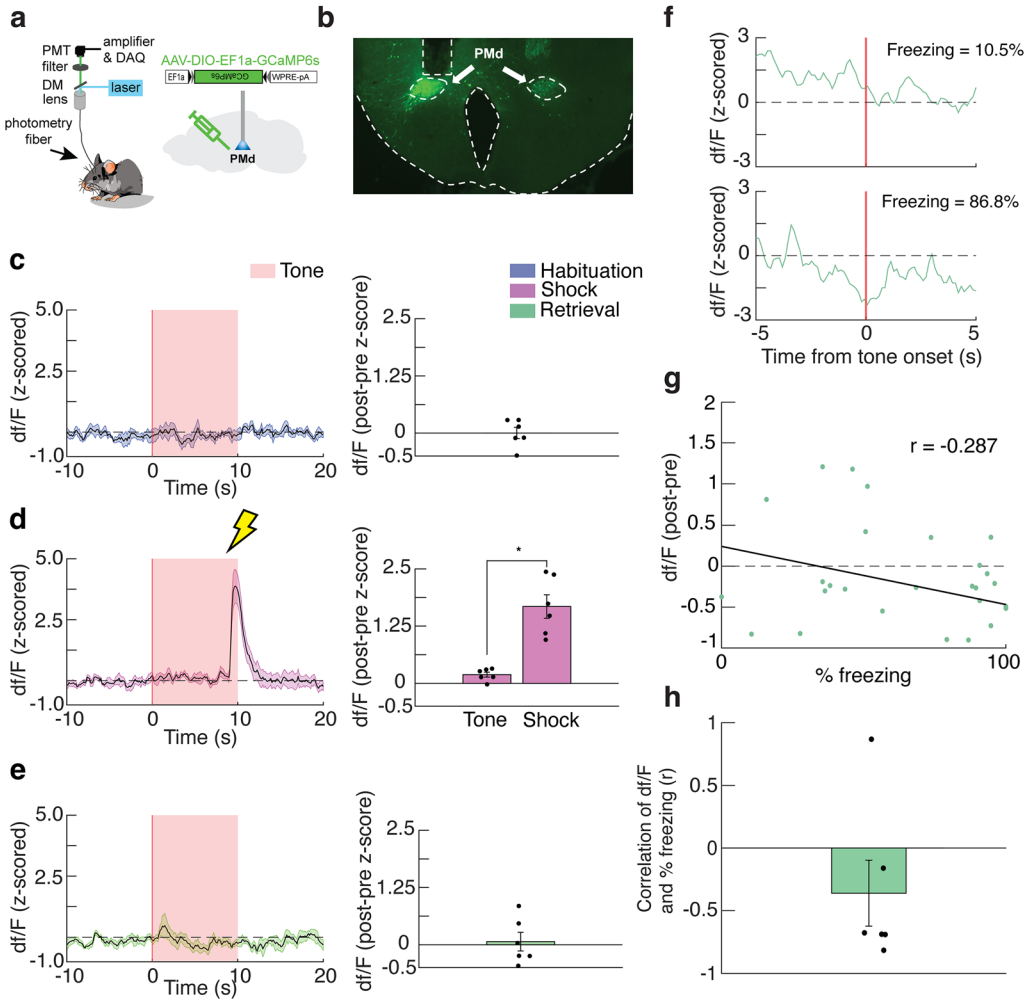

Figure 6. PMd-cck cells are not activated by a fear-conditioned auditory tone. Mice went through a 3 d auditory fear conditioning protocol. Subjects were exposed to tones on Day 1 (habituation), tone–shock pairing on Day 2 (shock day), and tones only on Day 3 (retrieval). Neural activity was recorded from PMd-cck cell expression GCaMP6s. ***a***, Scheme showing fiber photometry recording setup used to record neural activity in PMd-cck cells with the calcium indicator GCaMP6s (left). Right, A vector encoding cre-dependent GCaMP6s was injected in the PMd of cck-cre mice. ***b***, Expression of GCaMP6s in the PMd of cck-cre mice. ***c***, Left, Average neural activity traces of PMd-cck cells during tone presentation in habituation. Right, Quantification of the neural activity to the tone. (***d***) PMd-cck cells were activated by the shock, but not the tone on fear acquisition (shock day). The response to shock was larger than to tone (Wilcoxon sign rank test: $p < 0.031$). ***e***, Same as ***c***, but for fear retrieval day. ***f***, Example traces of PMd-cck activity in trials with low (top) and high freezing (bottom). ***g***, Scatterplot showing PMd-cck activity does not correlate with freezing. ***h***, Average correlation of freezing and PMd-cck df/F across mice. $n = 6$ mice.

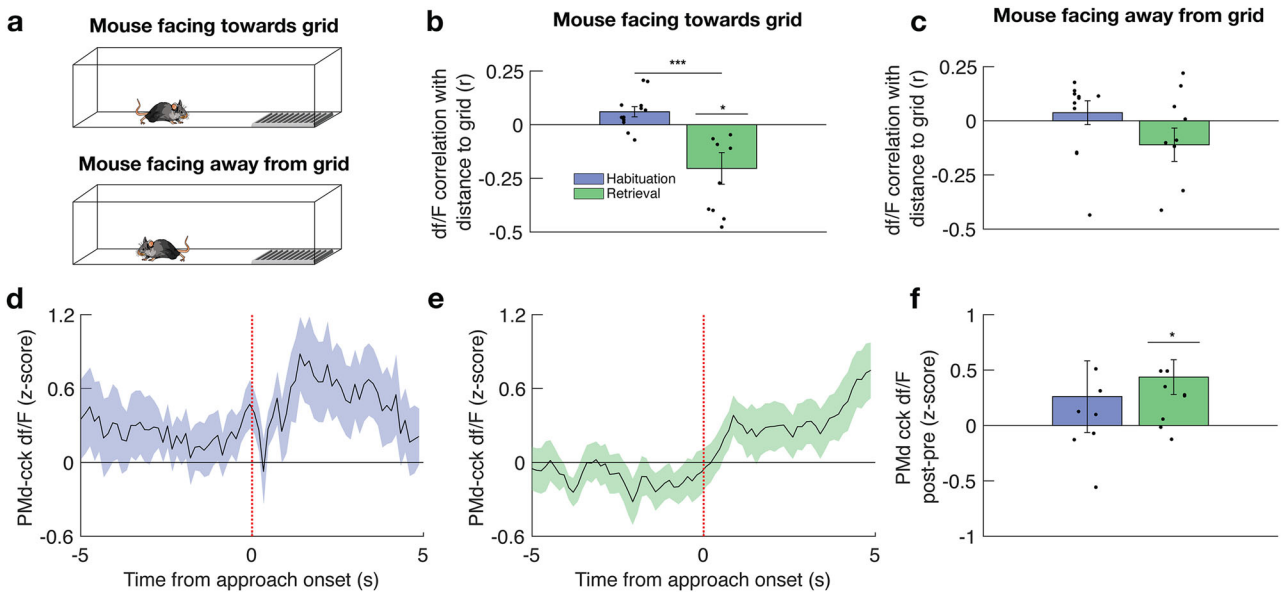

Figure 7. PMd-cck activity is correlated with stationary grid proximity in FUGA assay only when mice are facing the grid in the FUGA assay. ***a***, Scheme shows moments when the grid is stationary and the mouse is either facing toward the grid or away from the grid. Data plotted in ***b*** and ***c*** only include moments in which the grid is not moving, during the intertrial periods of the FUGA assay. ***b***, Correlation of df/F with distance to threat is significantly different from zero during retrieval while the mouse is facing the grid (angle between mouse head and grid is <30°; $*p = 0.0195$, Wilcoxon sign rank test). Correlation values are significantly different across days ($***p = 0.0027$, Wilcoxon rank sum test). ***c***, Same as left, but for moments in which the mouse is facing away from the grid (angle between mouse head and grid is >150°). ***d***, Average trace across mice showing PMd-cck activity centered at approach toward the shock grid in habituation day while the grid is stationary. ***e***, Average traces across mice showing PMd-cck activity increases when mice approaches the stationary grid during fear retrieval in the FUGA assay. ***f***, PMd-cck activity is significantly increased when mice approach the stationary shock grid in fear retrieval, but not habituation, of the FUGA assay ($p = 0.0137$, Wilcoxon sign rank test; data are plotted as mean ± SEM).

retrieval than in habituation, and thus this result cannot be induced by higher velocity in retrieval than in habituation, as only data points prior to the onset of successful FUGA were used.

Though these data only use time points prior to FUGA, it is possible that the PMd-cck activation seen near the grid in trials with successful FUGA (Fig. 8*e*,*f*, light green) is not related to grid proximity, but rather due to PMd activation in anticipation of the high-velocity FUGA escape that will happen in the near future. To address this confound, we show that in retrieval trials without successful FUGA, PMd-cck activity was also negatively correlated with distance to threat (Fig. 8*e*,*f* , FUGA fail trials in dark green). PMd activation was observed at grid movement onset even in FUGA fail trials which have the same mouse speed profile as in habituation (Extended Data Fig. 8-3 and Fig. 8*f*). Taken together, these results show that PMd-cck cells represent distance to the moving grid after, but not before, fear learning. Neural activity correlation with distance to grid was observed during retrieval trials with low speed prior to FUGA onset (due to high freezing), and this correlation is also seen during FUGA fail retrieval trials, which have speed similar to habituation during grid movement. These data indicate that the df/F and distance-to-grid correlation cannot be explained by overall locomotor differences across conditions.

We then investigated PMd-cck activity during FUGA escape, which occurs several seconds following grid movement onset (Fig. 8*c*). PMd-cck cells showed marked activation during FUGA escapes (Fig. 9*a*,*b*). These behaviors tend to have high speed, as the animal is escaping from a threat during FUGA. We thus investigated if the PMd activation seen during FUGA can be attributed to high general locomotion. We then compared data points from exploratory ambulation during habituation with data from matched speed ranges obtained from FUGA behavior during retrieval. Remarkably, PMd-cck activation was higher during retrieval FUGA escape than speed-matched exploration in habituation (Fig. 9*c*). These data show that PMd-cck cell activation during FUGA escape is specifically related to flight from threat, rather than general locomotion at the same speed range, as shown during other assays with escape (Wang et al., 2021a).

Interestingly, data from representative trials indicate that PMd-cck activity is correlated with FUGA speed (Fig. 10*a*–*c*). FUGA speed was correlated with PMd activity in retrieval, but not during habituation (Fig. 10*d*), suggesting that this effect was a consequence of fear learning. PMd activity and FUGA speed were correlated in late (last five trials of shock day), but not early shock day trials (first five trials with shock), indicating that this correlation is dependent on learning (Fig. 10*d*). Importantly, mouse velocity during FUGA is similarly high in both early and late shock trials (Fig. 10*e*), though neural activity is only correlated with speed in late shock trials. This analysis demonstrates that the observed correlation is not a direct consequence of high speed. Rather, the correlation between escape speed and neural activity only appears after learning, in late shock trials and retrieval trials. Furthermore, neural activity is not correlated with ambulatory exploration (Fig. 10*f*), but it is significantly correlated with FUGA speed (Fig. 10*g*) even when parsing the data into the same speed ranges for both exploration and FUGA. Lastly, we show that in these speed range-matched data PMd-cck activity is significantly higher in FUGA escape than in general exploratory locomotion (Fig. 10*h*). These data show that PMd-cck cells are correlated with FUGA speed, but not general locomotion.

Discussion

Summary of findings

Here, we describe FUGA, a novel assay to induce learned flight. In this paradigm, mice associate a moving shock grid with threatening footshocks and learn to rapidly traverse over the shock grid (FUGA behavior). Additionally, mice also show higher levels of

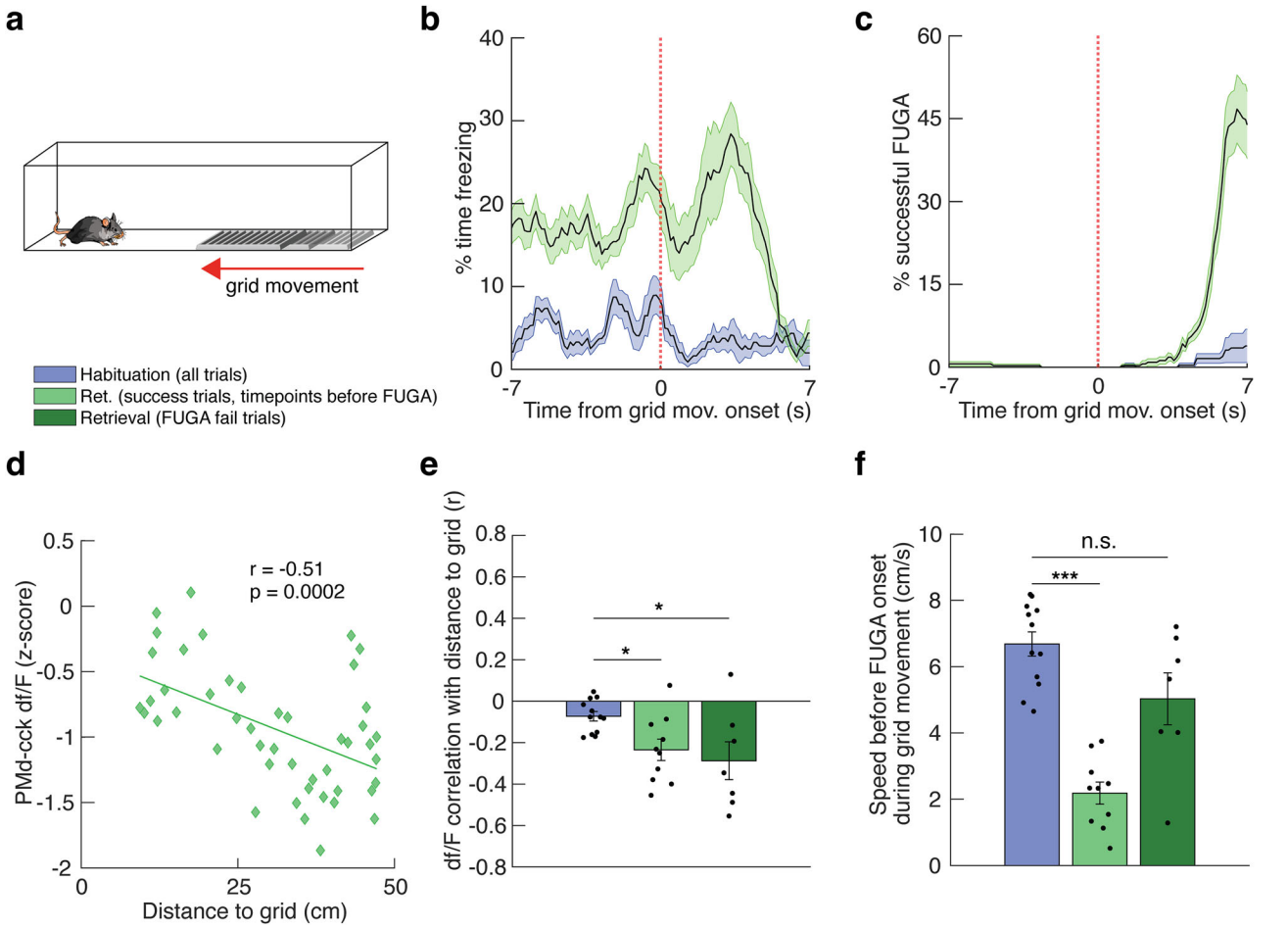

Figure 8. PMd-cck activity is higher during proximity to the moving shock grid. ***a***, Scheme showing grid movement epochs in the FUGA assay. ***b***, During grid movement, freezing is higher during retrieval than habituation. Freezing decreases in retrieval after several seconds of grid movement because mice start engaging in FUGA escape (***c***) as the grid nears the mouse. ***d***, Data from representative trial in retrieval showing that PMd-cck activity is negatively correlated with distance from the grid. The data in ***d*** are from grid movement time points in an example trial that occur prior to the onset of FUGA. ***e***, PMd-cck df/F is negatively correlated with distance to the grid in retrieval. Data from retrieval are separated into trials in which the mouse performed successful FUGA or failed to do so (light and dark green, respectively). For retrieval trials with successful FUGA, the correlation was calculated using data only prior to the onset of FUGA. For habituation and retrieval data with failed FUGA, all data during grid movement was used. Since time points with successful FUGA are excluded, these correlations are not affected by ongoing high-velocity FUGA escapes. The correlation in retrieval trials with and without FUGA is significantly lower than during habituation ($p = 0.011$ and $p = 0.028$, respectively, Wilcoxon rank sum test). ***f***, Average mouse speed during the grid movement prior to FUGA onset is lower in successful retrieval trials than in habituation trials ($p = 0.00008$, Wilcoxon rank sum test) because freezing is higher during retrieval than habituation (see Panel ***b***). Data are plotted as mean ± SEM ($n = 12$ habituation, 10 retrieval; Extended Data Figs. 8-1–8-3).

freezing and grid avoidance after fear acquisition. This assay exploits an ethologically relevant behavior in mice: rapid flight to evade an approaching threat, which is an action of paramount importance for survival. Remarkably, mice learn in a single session to perform FUGA and can retrieve this behavior in the absence of shock during the next day. We also show that PMd-cck activity is necessary for learning of the FUGA task (Fig. 3), but not contextual (Fig. 4) or auditory fear conditioning (Fig. 5), demonstrating that the PMd has a specific function in learning about moving threats. Furthermore, these cells represent learned FUGA escapes (Figs. 7–10), but not freezing in tone fear conditioning (Fig. 6). PMd-cck cells also represent threat imminence in this task, as shown in other hypothalamic circuits (Nguyen et al., 2024). Taken together, these data support a role for PMd-cck cells in the maintenance of the memory of the danger associated with a moving threat.

Novel FUGA assay

The most common protocols to study conditioned defense are auditory and contextual fear conditioning, in which the main measured behavior is freezing. Though freezing is a valuable metric, classical conditioning paradigms do not elicit other defensive actions such as escape. In the FUGA assay mice acquire in a single fear acquisition session a rich ethogram of defensive behaviors during retrieval, including avoidance, freezing, and learned flight (Fig. 2). This assay likely induces rapid learning because it simulates an ethologically relevant situation: the approach of a concrete and identifiable threat.

The FUGA assay recruits the PMd, a nucleus that coordinates reactions to high-imminence threats (Wang et al., 2021b) and that is activated by potential lethal danger, such as predators (Cezario et al., 2008; Wang et al., 2021a; de Araujo Salgado et al., 2023) and suffocation (Johnson et al., 2011). Thus, PMd involvement in this assay and the presence of flight thus suggest that grid approach elicits a perception of high threat imminence.

This assay also produces lower threat imminence epochs when the grid is more far away, which shifts the defensive actions from escape toward freezing and avoidance. Consequently, this assay provides a rich landscape to study circuits controlling distinct stages of the predatory imminence continuum

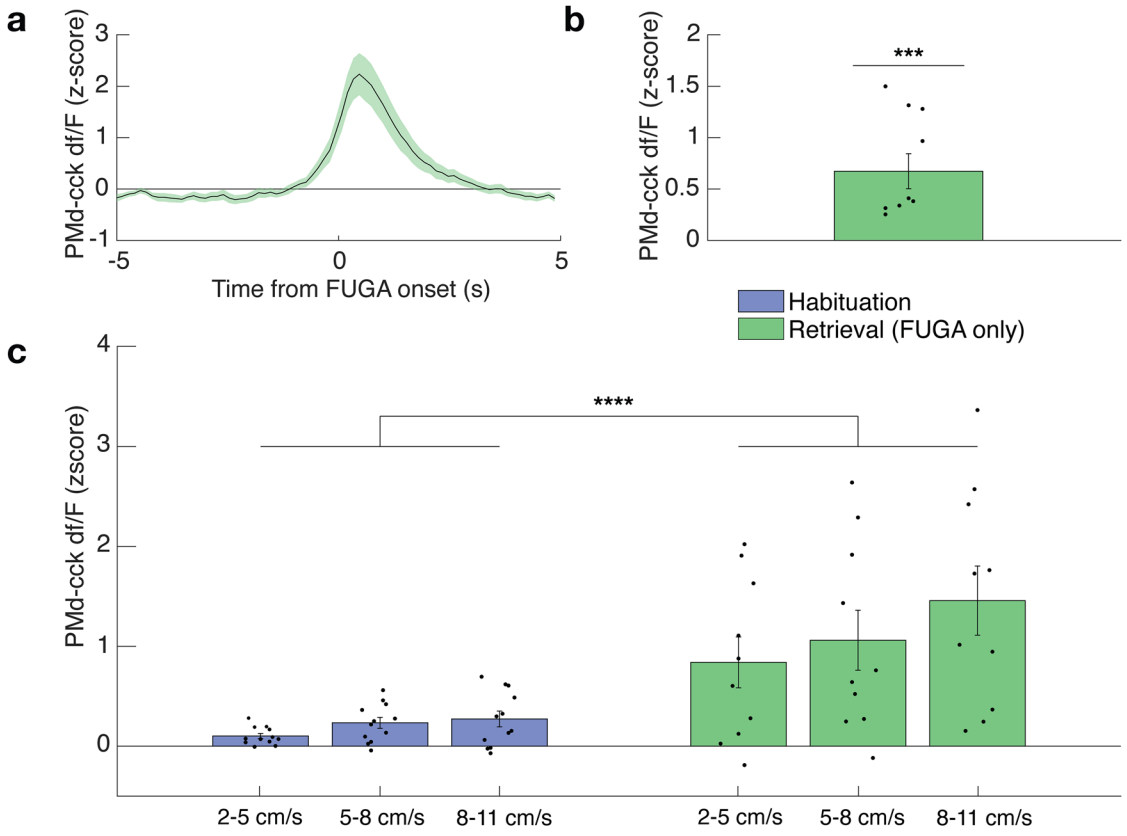

Figure 9. PMd-cck neurons are activated during conditioned FUGA escape compared with speed-matched exploratory behavior. ***a***, Average trace across mice showing that PMd-cck cells are activated during FUGA in retrieval. ***b***, Quantification of PMd-cck activation during FUGA escape in retrieval ($p = 0.0039$, Wilcoxon sign rank test). ***c***, Quantification of PMd-cck activity in ambulation in habituation and FUGA escape data points during retrieval that were selected in matched speed ranges. ****$p = 9.64 \times 10^{-7}$, $F = 29.79$, for ANOVA, main effect of day (habituation vs retrieval). Data are plotted as mean ± SEM ($n = 12$ habituation, $n = 10$ retrieval).

(Perusini and Fanselow, 2015), as well as providing moments in which behavioral strategies shift from freezing to flight.

Prior assays using predatory robots (Choi and Kim, 2010; Amir et al., 2015; Tsutsui-Kimura et al., 2022; Han et al., 2023; Lai et al., 2024) also produce escape and inhibit foraging. However, these assays cannot be used to study flight-related learning and memory. These assays are advantageous to study threat-induced inhibition of food-seeking and innate defensive actions, while the FUGA assay is better suited for investigating acquisition and retrieval mechanisms of learned flight.

An interesting aspect of the FUGA assay is the ability to parametrically control threat imminence by altering distance to threat. Threat proximity is a major factor influencing the topography of defensive behavior, but to the best of our knowledge, prior standard tasks did not have this feature. Future studies investigating the PMd or other circuits may alter the velocity or acceleration of the grid to identify how these factors affect behavior and neural dynamics.

PMd control of learned defensive actions

The PMd has been mostly studied due to its role in innate antipredatory defensive responses. Nevertheless, it also influences learned defense. For example, β-adrenergic activation of the PMd can induce conditioned odor aversion (Pavesi et al., 2011). Moreover, PMd inhibition decreases escape vigor during fear retrieval (Wang et al., 2021a), facilitates extinction of shock-induced contextual conditioning (Viellard et al., 2024), and decreases risk assessment in a context paired with prior social defeat (Faturi et al., 2014). Now, we show that PMd-cck inhibition during fear acquisition impairs learned flight during retrieval. Importantly, during shock day, PMd-cck inhibition did not alter any behavioral metrics (Extended Data Fig. 3-2), indicating that inhibiting these cells did not alter shock sensitivity or overall anxiety levels. Indeed, we have previously shown that PMd-cck activity was neither necessary nor sufficient for analgesia or innate anxiety (Wang et al., 2021b). These data indicate that the effects observed in retrieval following PMd-cck inhibition during shock day cannot be explained by overall changes in pain sensitivity or anxiety and thus are compatible with the view that PMd-cck cells have a role in the maintenance of learned escape or in the maintenance of the memory of threat levels associated with the moving grid.

Intriguingly, PMd-cck inhibition during FUGA acquisition impaired not only learned flight but also produced modest impairments in freezing and grid avoidance (Fig. 3*b*,*c*). These data thus indicate that while PMd activity is preferentially needed for the maintenance of the memory of the threat levels of the grid, it may also affect other conditioned defensive actions. Accordingly, a recent study showed that PMd-cck inhibition decreased conditioned freezing and avoidance during retrieval of contextual fear (Viellard et al., 2024). The PMd may also affect avoidance in situations containing both threats and rewards, as PMd-cck inhibition increases food intake and decreases avoidance of a predator (de Araujo Salgado et al., 2023). These results indicate that PMd activity during

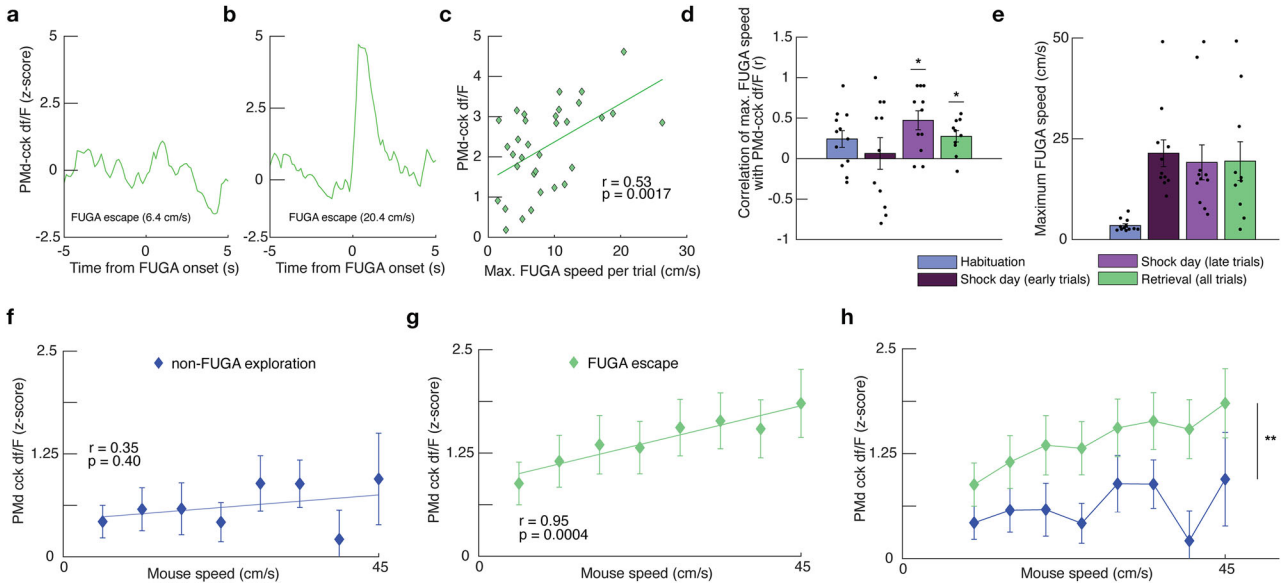

Figure 10. PMd-cck activity is correlated with FUGA escape vigor, but not general locomotion. Example PMd-cck neural activity traces from trials with low (***a***) and high (***b***) FUGA speed. Note that PMd-cck activity is higher in the trial with higher speed. ***c***, Representative data from example mouse showing that across all retrieval trial PMd-cck activity is positively correlated with FUGA speed. ***d***, Average correlations of PMd-cck activity with FUGA speed across the learning. ***d***, FUGA speed is positively correlated with PMd-cck activity in later shock day trials (last 5 trials during shock day) and during retrieval, but not during habituation or early shock day trials (first 5 trials of shock day). $p = 0.013$ and 0.0137 for the last five trials of shock and retrieval, respectively (Wilcoxon sign rank test). ***e***, FUGA speed is low during habituation, but not shock or retrieval days. Note that FUGA speed is not correlated with df/F prior to learning during the early shock day trials even though FUGA speed is high in these trials. ***f***, PMd-cck activity during retrieval of FUGA assay across different speed ranges for periods of exploratory locomotion without FUGA escapes. Neural activity was averaged across mice and binned in specific speed ranges ranging from 5 to 45 cm/s. Note that mouse speed is not significantly correlated with neural activity during general locomotion. ***g***, Same as ***f***, but for data points selected from FUGA escape moments (***f***). The scatterplot shows that mouse speed is significantly correlated with PMd-cck neural activity during FUGA. ***h***, PMd-cck activity is higher for the same speed ranges during FUGA escape compared with general exploratory locomotion ($F = 15.06$, $p = 0.0002$, repeated measures ANOVA). Data are plotted as mean ± SEM ($n = 12$ habituation, 10 retrieval).

acquisition and retrieval may affect a wide range of conditioned defensive actions extending beyond flight, even though the primary effect seen during optogenetic PMd-cck activation is flight, but not freezing (Wang et al., 2021b). Additionally, optogenetic activation of PMd-cck neurons triggers dynamic real-time place aversion (Wang et al., 2021b). This suggests that inhibiting PMd-cck cells may attenuate the aversive experience, potentially disrupting the stimulus-response associations critical for learning defensive actions necessary for adaptive avoidance in the FUGA assay.

It is unclear which PMd output projections are necessary for FUGA. Prior data indicate the PMd projection to the anterior medial ventral thalamus (Amv) may be important for learned defense, as Amv inactivation in rats with muscimol before exposure to a live cat predator, and not after, reduced contextual fear responses (de Lima et al., 2017). This result suggests the Amv controls the acquisition, but not retrieval of contextual fear associated with a predator. Considering that the Amv receives substantial input from the PMd (Canteras and Swanson, 1992), the distinct control of PMd → Amv of contextual escape suggests this circuit may control fear acquisition in the FUGA assay. Recent data showed that optogenetic inhibition of the PMd-cck → Amv projection accelerated extinction in a fear-conditioned context (Viellard et al., 2024), suggesting this projection may also control the extinction of behaviors seen in the FUGA assay.

Hypothalamic control of learning

A commonly held view is that the hypothalamus does not influence learning and that its main function is to control survival drives. Indeed, activation of neurons in the ventromedial hypothalamus induces potent aggression (Lin et al., 2011), while activation of lateral hypothalamus GABAergic cells elicits feeding (Jennings et al., 2013). However, emerging streams of data indicate that the hypothalamus can also potentially affect learning and memory (Burdakov and Peleg-Raibstein, 2020). Hypothalamic involvement in learning was noted many decades ago, as lateral hypothalamic lesions prevented the acquisition of taste aversion, but not the recall of prior taste aversion (Schwartz and Teitelbaum, 1974). More recent data show that hypothalamic neurons containing melanin-concentrating hormone (MCH) are active during the encounter of new objects. Silencing these cells during such encounters impairs recognition of these objects in later test sessions (Kosse and Burdakov, 2019). Such effects of MCH cells may be mediated by their dense projections to the hippocampus (Izawa et al., 2019). Accordingly, MCH cell activity is key for forgetting hippocampal-dependent memories during sleep (Izawa et al., 2019). Furthermore, lack of MCH receptors leads to impaired NMDA receptor function in the hippocampus, which may be a mechanism mediating the role of MCH cells in memory (Adamantidis et al., 2005). The activity of hypothalamic orexin neurons also affects memory, as activating them facilitates short-term spatial memory (Aitta-Aho et al., 2016) and enhances fear learning (Sears et al., 2013). Moreover, GABAergic neurons in the lateral hypothalamus have been shown to suppress learning about cues unrelated to rewards (Sharpe, 2024). Though studying hypothalamic involvement in learning is challenging in humans, there are reports of patients with hypothalamic damage displaying impaired memory recall (Ptak et al., 2001). The present data add to this growing body of evidence implicating the hypothalamus in learning and show that hypothalamic PMd-cck neurons also participate in learned behavioral aspects. Our results also show that this role

is specific to either maintaining learned FUGA escape or memory of the threat level induced by the moving grid. Future studies may determine which plasticity-related molecular pathways and which projections are involved in PMd influences in dependent learned actions.

References

Adamantidis A, et al. (2005) Disrupting the melanin-concentrating hormone receptor 1 in mice leads to cognitive deficits and alterations of NMDA receptor function. Eur J Neurosci 21:2837–2844.

Aitta-Aho T, Pappa E, Burdakov D, Apergis-Schoute J (2016) Cellular activation of hypothalamic hypocretin/orexin neurons facilitates short-term spatial memory in mice. Neurobiol Learn Mem 136:183–188.

Amir A, Lee S-C, Headley DB, Herzallah MM, Pare D (2015) Amygdala signaling during foraging in a hazardous environment. J Neurosci 35:12994–13005.

Borkar CD, et al. (2020) Sex differences in behavioral responses during a conditioned flight paradigm. Behav Brain Res 389:112623.

Borkar CD, et al. (2024) Top-down control of flight by a non-canonical cortico-amygdala pathway. Nature 625:743–749.

Burdakov D, Peleg-Raibstein D (2020) The hypothalamus as a primary coordinator of memory updating. Physiol Behav 223:112988.

Canteras NS, Swanson LW (1992) The dorsal premammillary nucleus - an unusual component of the mammillary body. Proc Natl Acad Sci U S A 89:10089–10093.

Canteras NS, Chiavegatto S, Ribeiro do Valle LE, Swanson LW (1997) Severe reduction of rat defensive behavior to a predator by discrete hypothalamic chemical lesions. Brain Res Bull 44:297–305.

Cezario AF, Ribeiro-Barbosa ER, Baldo MV, Canteras NS (2008) Hypothalamic sites responding to predator threats–the role of the dorsal premammillary nucleus in unconditioned and conditioned antipredatory defensive behavior. Eur J Neurosci 28:1003–1015.

Choi J-S, Kim JJ (2010) Amygdala regulates risk of predation in rats foraging in a dynamic fear environment. Proc Natl Acad Sci U S A 107:21773–21777.

de Araujo Salgado I, Li C, Burnett CJ, Rodriguez Gonzalez S, Becker JJ, Horvath A, Earnest T, Kravitz AV, Krashes MJ (2023) Toggling between food-seeking and self-preservation behaviors via hypothalamic response networks. Neuron 111:2899–2917.e6.

de Lima MAX, Baldo MVC, Canteras NS (2017) A role for the anteromedial thalamic nucleus in the acquisition of contextual fear memory to predatory threats. Brain Struct Funct 222:113–129.

Do Monte FHM, Canteras NS, Fernandes D, Assreuy J, Carobrez AP (2008) New perspectives on beta-adrenergic mediation of innate and learned fear responses to predator odor. J Neurosci 28:13296–13302.

Fanselow MS (2010) From contextual fear to a dynamic view of memory systems. Trends Cogn Sci 14:7–15.

Faturi CB, Rangel Jr MJ, Baldo MV, Canteras NS (2014) Functional mapping of the circuits involved in the expression of contextual fear responses in socially defeated animals. Brain Struct Funct 219:931–946.

Han H-B, Shin H-S, Jeong Y, Kim J, Choi JH (2023) Dynamic switching of neural oscillations in the prefrontal-amygdala circuit for naturalistic freeze-or-flight. Proc Natl Acad Sci U S A 120:e2308762120.

Izawa S, et al. (2019) REM sleep-active MCH neurons are involved in forgetting hippocampus-dependent memories. Science 365:1308–1313.

Jennings JH, Rizzi G, Stamatakis AM, Ung RL, Stuber GD (2013) The inhibitory circuit architecture of the lateral hypothalamus orchestrates feeding. Science 341:1517–1521.

Jercog D, et al. (2021) Dynamical prefrontal population coding during defensive behaviours. Nature 595:690–694.

Johansen JP, Tarpley JW, LeDoux JE, Blair HT (2010) Neural substrates for expectation-modulated fear learning in the amygdala and periaqueductal gray. Nat Neurosci 13:979–986.

Johnson PL, Fitz SD, Hollis JH, Moratalla R, Lightman SL, Shekhar A, Lowry CA (2011) Induction of c-Fos in "panic/defence"-related brain circuits following brief hypercarbic gas exposure. J Psychopharmacol 25:26–36.

Kosse C, Burdakov D (2019) Natural hypothalamic circuit dynamics underlying object memorization. Nat Commun 10:2505.

Lai AT, Espinosa G, Wink GE, Angeloni CF, Dombeck DA, MacIver MA (2024) A robot-rodent interaction arena with adjustable spatial complexity for ethologically relevant behavioral studies. Cell Rep 43:113671.

Lin D, Boyle MP, Dollar P, Lee H, Lein ES, Perona P, Anderson DJ (2011) Functional identification of an aggression locus in the mouse hypothalamus. Nature 470:221–226.

Maren S (2001) Neurobiology of Pavlovian fear conditioning. Annu Rev Neurosci 24:897–931.

Mathis A, Mamidanna P, Cury KM, Abe T, Murthy VN, Mathis MW, Bethge M (2018) Deeplabcut: markerless pose estimation of user-defined body parts with deep learning. Nat Neurosci 21:1281–1289.

McNaughton N, Corr PJ (2004) A two-dimensional neuropsychology of defense: fear/anxiety and defensive distance. Neurosci Biobehav Rev 28:285–305.

Nguyen QAT, Rocha A, Chhor R, Yamashita Y, Stadler C, Pontrello C, Yang H, Haga-Yamanaka S (2024) Hypothalamic representation of the imminence of predator threat detected by the vomeronasal organ in mice. bioRxivorg. https://pubmed.ncbi.nlm.nih.gov/37808690/

Pavesi E, Canteras NS, Carobrez AP (2011) Acquisition of Pavlovian fear conditioning using beta-adrenoceptor activation of the dorsal premammillary nucleus as an unconditioned stimulus to mimic live predator-threat exposure. Neuropsychopharmacology 36:926–939.

Perusini JN, Fanselow MS (2015) Neurobehavioral perspectives on the distinction between fear and anxiety. Learn Mem 22:417–425.

Ptak R, Birtoli B, Imboden H, Hauser C, Weis J, Schnider A (2001) Hypothalamic amnesia with spontaneous confabulations: a clinicopathologic study. Neurology 56:1597–1600.

Reis FMCV, et al. (2024) Control of feeding by a bottom-up midbrain-subthalamic pathway. Nat Commun 15:2111.

Schwartz M, Teitelbaum P (1974) Dissociation between learning and remembering in rats with lesions in the lateral hypothalamus. J Comp Physiol Psychol 87:384–398.

Sears RM, Fink AE, Wigestrand MB, Farb CR, de Lecea L, Ledoux JE (2013) Orexin/hypocretin system modulates amygdala-dependent threat learning through the locus coeruleus. Proc Natl Acad Sci U S A 110:20260–20265.

Shang CP, et al. (2018) Divergent midbrain circuits orchestrate escape and freezing responses to looming stimuli in mice. Nat Commun 9:1232.

Sharpe MJ (2024) The cognitive (lateral) hypothalamus. Trends Cogn Sci 28:18–29.

Tobias BC, Schuette PJ, Maesta-Pereira S, Torossian A, Wang W, Sethi E, Adhikari A (2023) Characterization of ventromedial hypothalamus activity during exposure to innate and conditioned threats. Eur J Neurosci 57:1053–1067.

Tsutsui-Kimura I, Uchida N, Watabe-Uchida M (2022) Dynamical management of potential threats regulated by dopamine and direct- and indirect-pathway neurons in the tail of the striatum. bioRxiv https://www.biorxiv.org/content/10.1101/2022.02.05.479267.full

Viellard JMA, et al. (2024) A subiculum-hypothalamic pathway functions in dynamic threat detection and memory updating. Curr Biol 34:2657–2671.e7.

Wang W, et al. (2021a) Dorsal premammillary projection to periaqueductal gray controls escape vigor from innate and conditioned threats. Elife 10:e69178.

Wang W, et al. (2021b) Coordination of escape and spatial navigation circuits orchestrates versatile flight from threats. Neuron 109:1848–1860.e8.

Wirsing AJ, Cameron KE, Heithaus MR (2010) Spatial responses to predators vary with prey escape mode. Anim Behav 79:531–537.

Yilmaz M, Meister M (2013) Rapid innate defensive responses of mice to looming visual stimuli. Curr Biol 23:2011–2015.